AD_____

Award Number: DAMD17-99-1-9086

TITLE: A Novel Pathway to Down-Regulate ErbB Signaling in Mammary Epithelial Cells

PRINCIPAL INVESTIGATORS: Lei Duan, M.D.
Hamid Band, M.D., Ph.D.

CONTRACTING ORGANIZATION: Brigham and Women's Hospital
Boston, Massachusetts 02115

REPORT DATE: January 2002

TYPE OF REPORT: Annual Summary

PREPARED FOR: U.S. Army Medical Research and Materiel Command
Fort Detrick, Maryland 21702-5012

DISTRIBUTION STATEMENT: Approved for Public Release;
Distribution Unlimited

The views, opinions and/or findings contained in this report are those of the author(s) and should not be construed as an official Department of the Army position, policy or decision unless so designated by other documentation.

20020912 048

REPORT DOCUMENTATION PAGE

Form Approved
OMB No. 074-0188

Public reporting burden for this collection of information is estimated to average 1 hour per response, including the time for reviewing instructions, searching existing data sources, gathering and maintaining the data needed, and completing and reviewing this collection of information. Send comments regarding this burden estimate or any other aspect of this collection of information, including suggestions for reducing this burden to Washington Headquarters Services, Directorate for Information Operations and Reports, 1215 Jefferson Davis Highway, Suite 1204, Arlington, VA 22202-4302, and to the Office of Management and Budget, Paperwork Reduction Project (0704-0188), Washington, DC 20503

1. AGENCY USE ONLY (Leave blank)	2. REPORT DATE	3. REPORT TYPE AND DATES COVERED
	January 2002	Annual Summary (31 Dec 00 - 31 Dec 01)

4. TITLE AND SUBTITLE
A Novel Pathway to Down-Regulate ErbB Signaling in Mammary Epithelial Cells

5. FUNDING NUMBERS
DAMD17-99-1-9086

6. AUTHOR(S)
Lei Duan, M.D.
Hamid Band, M.D., Ph.D.

7. PERFORMING ORGANIZATION NAME(S) AND ADDRESS(ES)
Brigham and Women's Hospital
Boston, Massachusetts 02115

E-Mail: lduan@rics.bwh.harvard.edu

8. PERFORMING ORGANIZATION REPORT NUMBER

9. SPONSORING / MONITORING AGENCY NAME(S) AND ADDRESS(ES)
U.S. Army Medical Research and Materiel Command
Fort Detrick, Maryland 21702-5012

10. SPONSORING / MONITORING AGENCY REPORT NUMBER

11. SUPPLEMENTARY NOTES
Report contains color.

12a. DISTRIBUTION / AVAILABILITY STATEMENT
Approved for Public Release; Distribution Unlimited

12b. DISTRIBUTION CODE

13. ABSTRACT *(Maximum 200 Words)*

Activation of tyrosine kinases plays a key role in cell proliferation, and ErbB receptor tyrosine kinases are specifically implicated in breast cancer. Biochemical studies have recently identified the proto-oncogene product Cbl as a negative regulator of EGF receptor and ErbB2. The Cbl-dependent negative regulation of ErbB receptors was associated with their ubiquitin modification and down-regulation from the cell surface. Based on these observations, this proposal is investigating the role of Cbl-mediated ubiquitination as a signal for targeting activated ErbB receptors to lysosomes where they undergo degradation. The work reported here has demonstrated that ubiquitin modification of EGFR is essential for its down-regulation. Furthermore, this modification is shown to be essential for EGFR trafficking between early and late endosome, while being dispensable for initial endocytosis. Further studies aim to establish a causal role of Cbl in this process, using Cbl non-binding EGFR mutants that have been engineered and Cbl-deficient cell lines expressing EGFR or ErbB2 that have been generated. The present studies, thus, aim to understand the molecular basis of a novel pathway that controls the down-regulation of proliferative signals in breast cancer cells. Elucidation of this pathway is likely to reveal novel targets to develop rational therapeutic agents for breast cancer.

14. SUBJECT TERMS	15. NUMBER OF PAGES
breast cancer, signal transduction, epidermal growth factor receptor, ErbB2, tyrosine kinases, oncogenes	25
	16. PRICE CODE

17. SECURITY CLASSIFICATION OF REPORT	18. SECURITY CLASSIFICATION OF THIS PAGE	19. SECURITY CLASSIFICATION OF ABSTRACT	20. LIMITATION OF ABSTRACT
Unclassified	Unclassified	Unclassified	Unlimited

Table of Contents

A Novel Pathway to Down-Regulate ErbB Signaling in Mammary Epithelial Cells

Introduction:

The experiments proposed in this application are designed to test a unique hypothesis that the proto-oncogene product Cbl down-regulates ErbB by controlling its ligand-induced ubiquitination, internalization and degradation. Genetic studies, initially in C. elegans and Drosophila systems and recently using mouse knock-outs, as well as extensive biochemical studies have established Cbl as a negative regulator of tyrosine kinases. At the time of this application, the TKB domain of Cbl had been shown to be crucial for Cbl function, which formed the basis for the use of TKB domain mutants in our studies. Subsequent studies in our laboratory demonstrated that the RING finger domain of Cbl was crucial for negative regulation of EGFR and Syk tyrosine kinases. Furthermore, the TKB and RING finger domain (together with short conserved regions surrounding the RING finger domain) were sufficient for Cbl-induced negative regulation of EGFR and Syk, as well as for Cbl-mediated ubiquitination of EGFR. Given the ability of Cbl to support the ubiquitination of target proteins in vitro, the TKB and RING finger domains of Cbl together define a novel ubiquitin ligase module that specifically targets activated tyrosine kinases like ErbB receptors for ubiquitination. Understanding the mechanisms of this novel biochemical machinery and how ubiquitin modification mediates the negative regulation of ErbB receptors is likely to provide crucial insights of biological and medical significance.

Body:

Studies carried out in the current reporting period helped further the training of the trainee, and established that the ubiquitin modification of EGF receptor plays an essential role in its lysosomal targeting but not in the initial internalization. In addition, a number of EGFR mutants, Cbl-/- mouse embryonic fibroblast cell lines and their EGFR and ErbB2 transfectants have been generated for further studies.

Generation of CHO-TS20-EGFR cells for regulated EGFR ubiquitination. While recent studies, carried out by our laboratory and others, have demonstrated a tight correlation between Cbl-dependent ubiquitination of EGFR, a causal role of the ubiquitination in Cbl-mediated EGFR down-regulation has not been established. To formally assign a causal role for the ubiquitin pathway in EGFR down-regulation, we have used a genetic system in which the ubiquitination can be controlled. A Chinese Hamster Ovary (CHO) cell line TS20, established previously (Strous GJ, et al. EMBO J. 15:3806-3812, 1996), carries a temperature-sensitive mutant ubiquitin-activating enzyme (E1) that is functional at 30°C (permissive temperature) but nonfunctional at 42°C (non-permissive temperature). The E1 enzyme in the parental CHO cell line E36 is functional at both temperatures. This pair of cell lines was obtained from Dr. Ger Strous (University of Utrecht, Netherlands) and both cell lines were transfected with pCDNA3-EGFR followed by G418 selection to establish stable transfectant clones.

Immunoblotting with anti-EGFR antibodies was used to identify EGFR-expressing cells and these were used for further analyses.

First, we examined if inactivation of the ubiquitin machinery in these cells would abrogate the ligand-induced ubiquitination of EGFR. For this purpose, the cells were either left at the permissive temperature or shifted to the non-permissive temperature for 4 hours prior to EGF stimulation. The cell lysates were subjected to immunoprecipitation with an ant-EGFR antibody followed by anti-ubiquitin immunoblotting to detect the ubiquitinated EGFR. As anticipated, EGF stimulation of both the TS20-EGFR and E36-EGFR cell lines at the permissive temperature resulted in EGFR ubiquitination (**Fig. 1**). When cells were shifted to the non-permissive temperature, the EGF-induced ubiquitination of EGFR was still observed in E36-EGFR cells; in contrast, the EGFR ubiquitination was nearly completely abrogated in TS20-EGFR cells under identical conditions. Thus, inactivation of E1 in TS20 cells effectively inhibited the ligand-induced ubiquitination of EGFR.

Next, we examined if abrogation of the EGF-induced ubiquitination of EGFR resulted in inhibition of its degradation, as predicted by our hypothesis. For this purpose, the cells were stimulated as above for the ubiquitination studies but with a more prolonged time course to assess the loss of EGFR protein signal as a result of its induced degradation. As expected, EGF stimulation of TS20-EGFR as well as E36-EGFR cell lines at the permissive temperature resulted in a time-dependent loss of EGFR, with nearly complete degradation by 4 hours. Notably, when TS20-EGFR cells were shifted to the non-permissive temperature, a substantial delay in EGFR degradation was observed; a significant level of EGFR was detectable even at 4 hours of EGF stimulation (**Fig. 2**). In contrast, when E36-EGFR cells were examined at the non-permissive temperature, EGFR degradation was not inhibited; if anything, a faster degradation was observed. Thus, ubiquitin modification of EGFR is essential to promote its degradation, a process critical for EGFR down-regulation. Notably, these studies were carried out without exogenous Cbl over-expression, unlike previous studies.

An important question that our hypothesis proposed to ask was: at what level does the Cbl-dependent ubiquitination of EGFR operate? Previous studies have suggested that Cbl facilitates the trafficking of the activated EGFR into lysosomes; however, as ubiquitin serves as a signal for initial endocytosis of other receptors (e.g., the alpha factor receptor in yeast and mammalian growth hormone receptor) (Hicke L, Cell 106:527-530, 2001; Strous GJ, et al. EMBO J. 15:3806-3812, 1996), it has been unclear whether Cbl regulates the initial endocytosis or a later sorting event that directs the EGFR into the lysosomal as opposed to the recycling pathway. We have addressed this question in two ways, as described below: fluorescence-activated cell sorter (FACS)-based analysis of EGF internalization; and confocal microscopy of EGFR localization.

Internalization of EGFR is unaffected by abrogation of ubiquitination. To assess the role of EGFR ubiquitination in ligand-induced internalization step, we utilized a FACS-based assay. First, we established that the assay detects only the internalized EGFR. When Alexa-488-conjugated EGF was allowed to bind to E36-EGFR or TS20-

EGFR cells at 4°C, the bound EGF could be detected as a shift in the peak of fluorescence in FACS staining (**Fig. 3**, top panels versus third panels); however, an acid wash (which removes non-internalized EGF) essentially completely eliminated the fluorescence signals, as expected (**Fig. 3**, second panels versus top panels). In contrast, when fluorescent EGF was added to TS20-EGFR or E36-EGFR cells at 30°C for various time points, a time-dependent increase in acid-resistant fluorescence signal (due to internalized EGF) was seen; shifting of cells to 42°C did not lead to any diminution of EGF internalization in either E36-EGFR cells or TS20-EGFR cells (**Fig. 3**). Thus, abrogation of EGFR ubiquitination has no impact on its internalization into the cell, suggesting that inhibition of EGFR degradation under these conditions must reflect a block in lysosomal targeting rather than the initial endocytic process.

Confocal immunofluorescence (CIF) co-localization of EGFR and transferrin in CHO-TS20-EGFR cells indicates a requirement for ubiquitination in EGFR traffic from early to late endosomes: To further characterize the nature of the block on EGFR degradation imposed by lack of ubiquitination, we carried out confocal immunofluorescence microcopy (**Fig. 4**). When TS20-EGFR or E36-EGFR cells grown at 30°C were exposed to EGF for various time points and the localization of EGFR examined by CIF, it was clear that EGF induced a redistribution of EGFR from its initial cell surface location to intracellular vesicles. Two-color analysis showed co-localization of EGFR with labeled transferrin, a marker of early and recycling endosomes, at 10 minutes; however, this co-localization was significantly lost at 30 minutes, consistent with the movement of internalized EGFR into the late endosome/lysosome compartments. Importantly, when TS20-EGFR cells were examined at 42°C, the surface EGFR was efficiently internalized and co-localized with transferrin at 10 minutes; this result confirmed the FACS analyses presented above, indicating that lack of ubiquitination does not inhibit the internalization of EGFR. Notably, however, EGFR continued to co-localize with transferrin even at 30 minutes, indicating that lack of ubiquitination resulted in loss of progression of EGFR into the late endosome/lysosome compartment.

The potential role of ubiquitin modification as an endocytic trafficking signal is thought to involve mon- or di-ubiquitin modification (Hicke et al, above). To assess if Cbl-mediated ubiquitination of EGFR results in such a modification, we generated a yellow fluorescent protein tagged ubiquitin (YFP-Ub) expression plasmid and verified it ability to direct the expression of a protein of correct size in transfected cells (**Fig. 5-A**). The largere size of this protein allows unambiguous resolution of mono and di-ubiquitinated EGFR in SDS-PAGE. When YFB-Ub was used in co-transfection analyses, Cbl-dependent EGF-induced ubiquitin modification of EGFR in the form of mon- and di-ubiquitination was observed (**Fig. 5-B**). These results are further consistent with our hypothesis that Cbl-dependent ubiquitination results in endocytic traffic of EGFR to the lysosomal compartment.

Generation of EGFR mutants defective for Cbl-dependent ubiquitination: As an independent approach to demonstrate the role of ubiquitination in intracellular traffic of EGFR, and to assess the importance of Cbl in this process, we have generated EGFR

mutants that lack Cbl docking sites. Cbl TKB domain binds to pY1045 in EGFR (Waterman H, et al. EMBO J. 21:303-313, 2002), whereas the proline-rich region on Cbl mediates an indirect interaction with EGFR, via Grb2; Grb2 associates with Cbl proline-rich sequences via its SH3 domains and with EGFR pY1068 via its SH2 domain (Fukazawa T et al. J Biol. Chem. 271:14554-14559, 1996; Waterman H, et al. EMBO J. 21:303-313, 2002). Thus, we have generated EGFR constructs in the pAlterMAX vector that encode Y1045F, Y1068F and Y1045/1068F double mutant proteins. In initial analyses using transfection in 293T cells, we have established that Y1045F and Y1045/1068F mutants are defective in Cbl-dependent ubiquitination compared to the wildtype EGFR, whereas Y1068F mutant is not defective (**Fig. 6**). Thus, the TKB domain-mediated interaction of Cbl with EGFR is crucial for Cbl-dependent ubiquitination. These mutants will be further analyzed to confirm the conclusions derived from above studies and to identify the intracellular compartments where Cbl-dependent EGFR sorting taking place. For our further studies, we have also cloned these mutants in the pCDNA3 (neo^r) plasmid vector and in the pMSCV-blast retroviral vector ($blasticidin^r$) so that these can be stably expressed. The-pMSCV-blast was assembled in the laboratory from pEF-blast and pMSCV-hygro vectors, and its ability to impart blasticidin resistance on transfected cells has been verified

Establishment of Cbl+/+ and Cbl-/- MEFs from two distinct knockout models: As a critical test of our hypothesis that EGFR down-regulation is controlled by Cbl-dependent ubiquitination, we have sought to compare Cbl-expressing and Cbl-non-expressing cells of identical genetic background. For this purpose, we have generated MEF lines from Cbl-/- mice, together with their wild-type controls (**Fig. 7**). Cbl-/- mice have been generated by two different groups; in one case (Bowtell Lab), an aberrant, likely non-functional, Cbl protein is expressed at low levels (Murphy MA et al. Mol. Cell. Biol. 18:4872-4882, 1998). We have shown that Cbl deficiency in 'Bowtell' Cbl-/- MEFs leads to reduced ubiquitination and accumulation of Src-family kinases Fyn and Lck (2, 86, 88). To avoid possible problems due to low levels of aberrant Cbl, we have also derived a Cbl-/- MEF line (together with Cbl+/+ control) from mice generated by Dr. Hua Gu at the NIH (Naramura M et al. Proc. Natl. Acad. Sci. USA 95:15547-15552, 1998) (**Fig. 7**).

We further examined the Cbl-/- mouse embryo fibroblast (MEF) cell lines derived from these two Cbl-/- mouse strains (DB, from David Bowtell; GU, from Hua Gu) to characterize the status of expression of other Cbl family members. To assess the expression of Cbl-b, we utilized an antibody H454 (sc-1705 from Santa Cruz Biotechnology, Inc). Although promoted by Santa Cruz Biotechnology, Inc. as an anti-Cbl-b reagent, we have used transfected, epitope-tagged Cbl and Cbl-b proteins to establish that H-454 recognizes both Cbl and Cbl-b (**Fig. 8**). First, we carried out anti-Cbl IPs from our Cbl+/+ and Cbl-/- cells under conditions that completely immuno-depleted Cbl protein present in these lysates. We then used the depleted lysate for a second round of IPs with H454 antibody to pull down Cbl-b. Both set of IPs were resolved by SDS-PAGE and immunoblotted with H-454 antibody (**Fig. 9**). As expected, anti-Cbl IP from Cbl+/+ cells showed a prominent H-454-reactive band (Cbl), which was absent in anti-Cbl IPs from Cbl-/- cells. H-454 IP of Cbl-precleared lysates showed low

levels of Cbl-b (seen as a doublet) in both Cbl+/+ cell lines and in Cbl-/- DB cell line; this band was nearly undetectable in Cbl-/- GU MEF line (the reasons for complete lack of expression in this line are not known). The relative signals of Cbl and Cbl-b detected with H-454 blot suggest that only a low level of Cbl-b is expressed in these cell lines. These results were further confirmed by Northern blot analysis, which also revealed lack of Cbl-c mRNA expression in all MEFs (not shown). Overall, our results indicate that Cbl-/- MEFs that we have established express low to undetectable levels of Cbl family members, suggesting that these reagents will be useful for our analyses.

Establishment of EGFR and ErbB2-expressing Cbl+/+ and Cbl-/- MEF cell lines. As the endogenous EGFR levels in MEFs are low, we have established stable transfectants of the two pairs of MEFs expressing the human EGFR or ErbB2. For this purpose, human EGFR and ErbB2 cDNAs were cloned in the pMSCV-puro retroviral vector and retroviral supernatants were generated by transient transfection in the packaging cell line Tsa... These retroviral supernatants were used to infect the Cbl+/+ and Cbl-/- MEFs, and stable transfectants were selected in puromycin. The expression of introduced EGFR or ErbB2 was examined using two separate analyses. First, immunoblotting of whole cell lysates (for ErbB2) or anti-EGFR immunoprecipitates (for EGFR) was used to confirm the expression of the introduced ErbB2 or EGFR (**Fig. 10 and 11**). Secondly, FACS analysis with human EGFR or ErbB2-specific monoclonal antibodies was used to demonstrate that the introduced receptors were expressed on the cell surface, and that the transfected cells expressed the introduced receptors in a relatively homogeneous manner (**Fig. 12 and 13**). We will reconstitute Cbl expression in the EGFR or ErbB2-transfected Cbl-/- MEFs, using retroviral infection with MSCV-hygro-HA-Cbl to derive two series of MEF lines (WT, Cbl-/- and Cbl-reconstituted) to directly assess if the endogenous Cbl protein is indeed essential for ubiquitination and down-regulation of ErbB receptors, EGFR and ErbB2. Experiments with ErbB2 represents an important extension of our studies as these are likely to provide important insights into the mechanism of action of Herceptin and other therapeutic antibodies that induce the down-regulation of this receptor.

Key Research Accomplishments:

- Generated a panel of new EGFR mutants carrying mutations in the Cbl docking sites in plasmid and retroviral vectors.
- Generated Cbl+/+ and Cbl-/- MEFs and their EGFR and ErbB2 transfectants.
- Generated stable EGFR transfectants of wildtype and mutant CHO cells carrying a temperature-sensitive mutation in the ubiquitin attachment machinery.
- Generated a yellow fluorescent protein-tagged ubiquitin (YFP-Ub) expression plasmid.

- Demonstrated an essential role for EGFR ubiquitination in its degradation, using a genetic approach.

- Demonstrated that EGFR ubiquitination is not required for initial internalization

- Demonstrated that lack of ubiquitination of EGFR results in its failure to traverse from early to late endosome.

- Demonstrated that Cbl-dependent EGFR ubiquitination involves predominantly mono- and di-ubiquitin modifications.

Reportable Outcomes:

Publications:

- **Duan L,** Miura Y, Dodge I, Dimri M, Fernandes N and Band H. EGFR ubiquitination is required for its endosome to lysosome traffic but not for internalization. Manuscript under preparation.

Reagents:

- Generated a panel of new EGFR mutants carrying mutations in the Cbl docking sites in plasmid and retroviral vectors.

- Generated Cbl+/+ and Cbl-/- MEFs and their EGFR and ErbB2 transfectants.

- Generated stable EGFR transfectants of wildtype and mutant CHO cells carrying a temperature-sensitive mutation in the ubiquitin attachment machinery.

- Generated a yellow fluorescent protein-tagged ubiquitin (YFP-Ub) expression plasmid.

Funding applied for based on this work:

The work carried out under this award is part of the background and preliminary studies for two NIH RO1 applications (Molecular Control of EGF Receptor Down-Regulation; PDGF Receptor Regulation by Cbl) submitted by Dr. Band, and are under review for June 2002 cycle.

Manuscripts included:

- None

Conclusions:

In conclusion, our results provide genetic evidence for an essential role of ubiquitination in EGFR down-regulation. Our results establish that ubiquitination plays an essential role for EGFR traffic from early endosome to late endosome, but is dispensable for initial endocytosis. Through our studies, we have also established Cbl+/+ and Cbl-/- cell lines and their EGFR and ErbB2 transfectants to directly establish that Cbl is indeed the controller of EGFR ubiquitination and down-regulation.

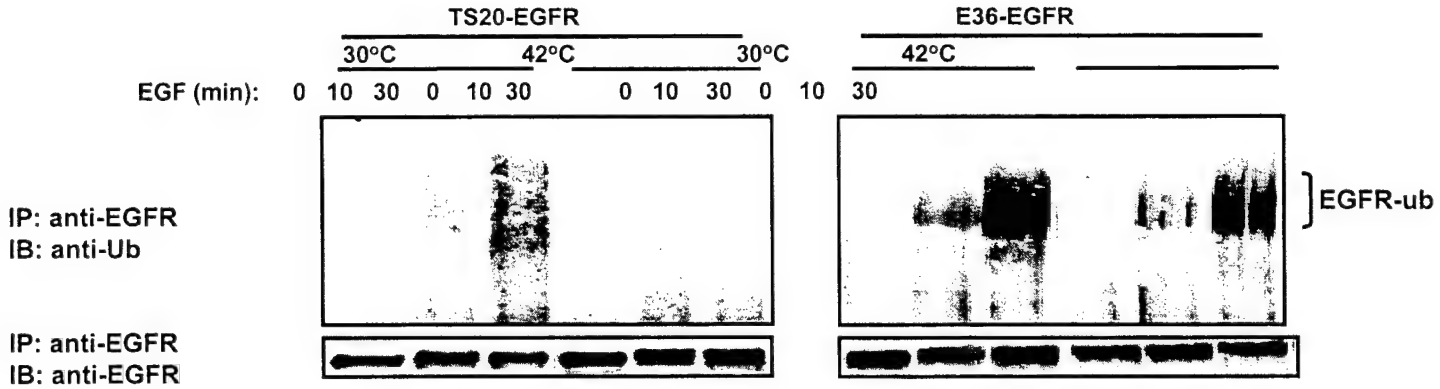

Figure 1. Temperature-regulated ubiquitination of EGFR in EGF-stimulated CHO-TS20-EGFR cells. The parental CHO-E36 and temperature sensitive CHO-TS20 cells were stably transfected with WT EGFR (E36-EGFR and TS20-EGFR, respectively). Subconfluent monolayers were either cultured at the permissive temperature (30°C) or shifted to the nonpermissive temperature (42°C) for 4 hr, subjected to a further 4 hr incubation in medium with 0.5% FBS media, and then stimulated with EGF (100ng/ml) for the indicated time. Anti-EGFR IPs were blotted with anti-Ub and anti-EGFR antibodies. Note that TS20-EGFR cells show EGFR ubiquitination only at 30°C whereas E36-EGFR cells show ubiquitination at 30°C as well as 42°C.

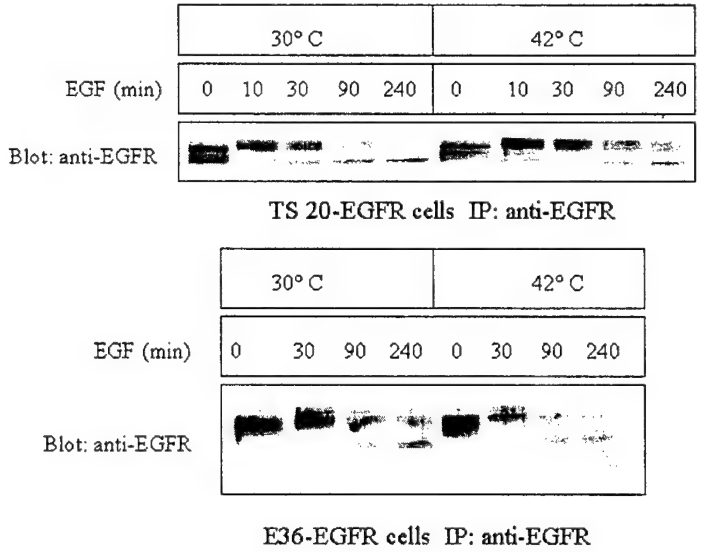

Fig. 2. Intact ubiquitination machinery is essential for EGF-induced degradation of EGFR. TS20-EGFR (upper panel) and E36-EGFR cells (lower panel) stably expressing EGF receptors were swtiched to 30°C or 42°C for 4 hours before stimulation, as indicated. The cells were then incubated with EGF (100 ng/ml) for the indicated time points before preparing lysates in 1% Triton X-100 lysis buffer. 50 μg aliquots of lysate protein were resolved by SDS PAGE, transferred to a PVDF membrane, and immunoblotted with an anti-EGFR antibody (sc003, Santa Cruz).

Fig. 3. CHO-TS20-EGFR (A) or CHO-E36-EGFR cells were plated on 10-cm culture dishes and grown for at 30° C for 48 hours until they reached about 75% confluence. The cells were then switched to 30° C or 42° C, as indicated at the top of figure panels. To assess cell surface binding (top two panels in each figure), cells were placed on ice and Alexa-488 conjugated EGF (100ng/ml; Molecular Probes, Inc.) in starving medium was added for 30 minutes. The cells were then washed and processed for FACS analysis to detect the total surface binding (top row in each figure). A duplicate plate of Alexa-488-stained cells was subjected to acid wash (0.2M acetic acid, 0.5M NaCl, pH 2.8) to remove the cell surface bound EGF to measure non-specific binding (second row in each figure). To measure the internalization of EGF, Alexa-fluo488 conjugated EGF was added to cells cultured at 30° C or 42° C and incubation continued at the same temperature for the indicated time points. At each time point, the cells were placed on ice and subjected to acid wash to remove the cell surface bound, non-internalized pool of EGF. The washed cells were then subjected to FACS analysis to detect the internalized fraction of EGF. FACS analysis was performed on a FACSort (Becton-Dikinson) and analyzed using the CellQuest program. For each histogram, the X-axis represents fluorescence intensity in log intervals and the Y-axis represents the cell numbers. 10,000 events were analyzed for each sample. The cursor designated M1 was placed to include cells that were right of the negative control (without Alexa-488 EGF staining). For each sample, the percent of cells shifting to right within the M1 gate were scored as positive and are shown on the right side of each panel. The mean fluorescence intensity (MFI) corresponds to fluorescence intensity of all cells, including the small negative population that remained unstained; the latter represents a small percentage of EGFR-negative cells in the transfectant at the time of analysis (a result of loss of transfected EGFR during long term culture). Please note that both TS20-EGFR and E36-EGFR internalize EGF at both the permissive and non-permissive temperatures.

Fig. 3A.

TS20-EGFR	30 ° C	% +, MFI	42° C	% +, MFI
Total surface Binding	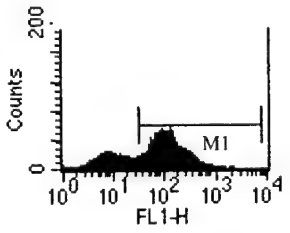	72, 102	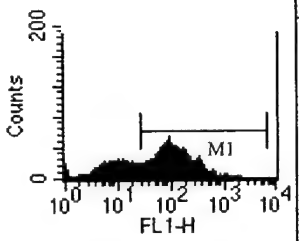	74 , 72
Background Binding	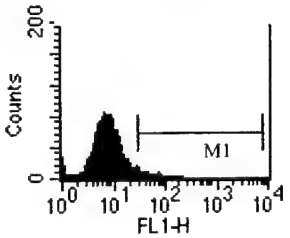	3.8, 9.8	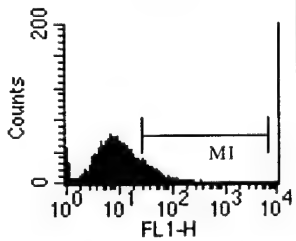	5.2, 11
Internalized				
Control	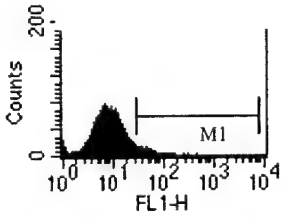	4.3, 11	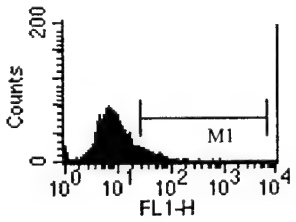	2.6, 9
EGF, 3 min	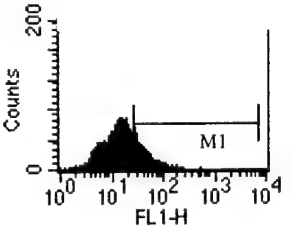	17, 19	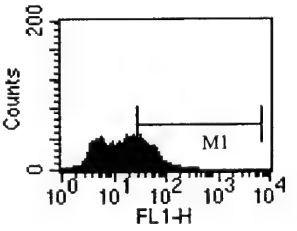	36, 26
EGF, 5 min	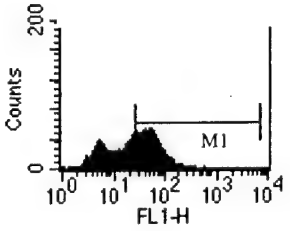	46, 34	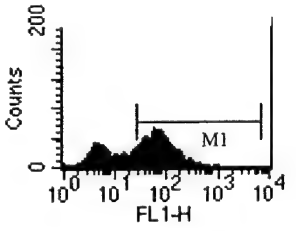	69, 58
EGF, 10 min	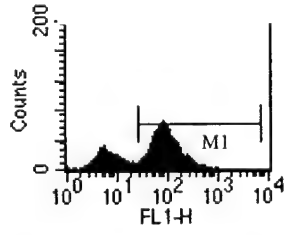	72, 73	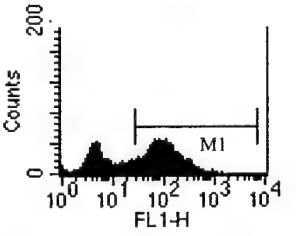	71, 70

Fig. 3B.

E36-EGFR

	30 ° C		42° C	
		% +, MFI		% +, MFI
Total Surface Binding	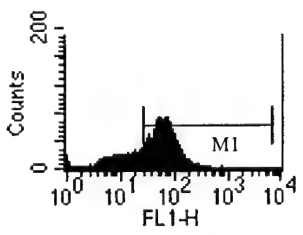	70, 53	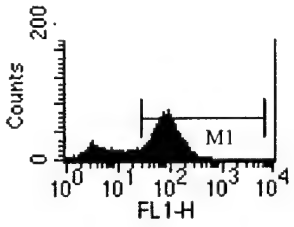	74, 71
Background Binding	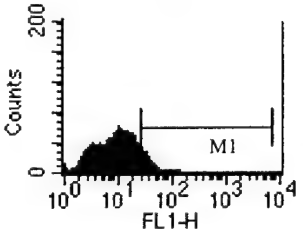	6, 12	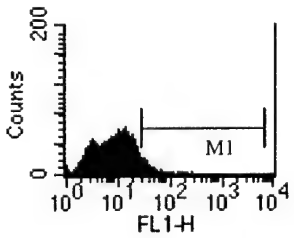	5, 11
Internalized				
Control	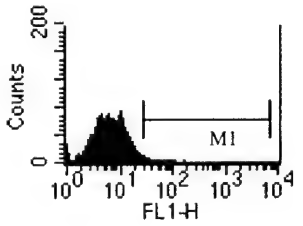	1.3, 8	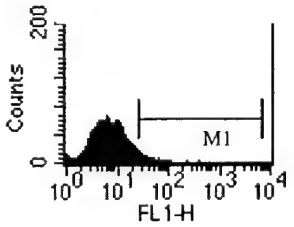	2.6, 9
EGF, 3 min	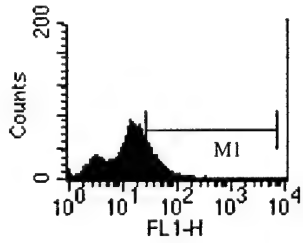	14, 17	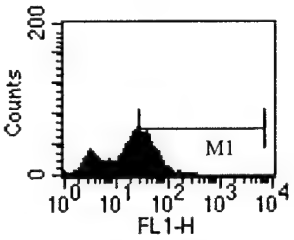	36, 26
EGF, 5 min	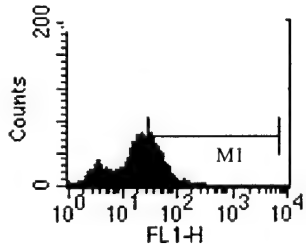	30, 24	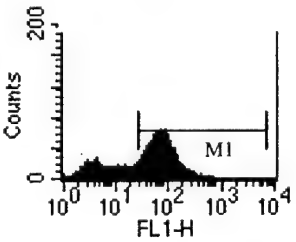	69, 58
EGF, 10 min	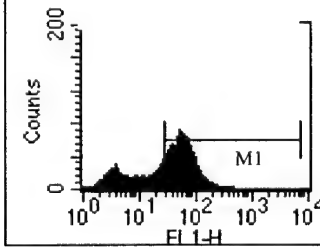	65, 44	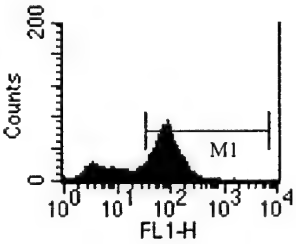	71, 70

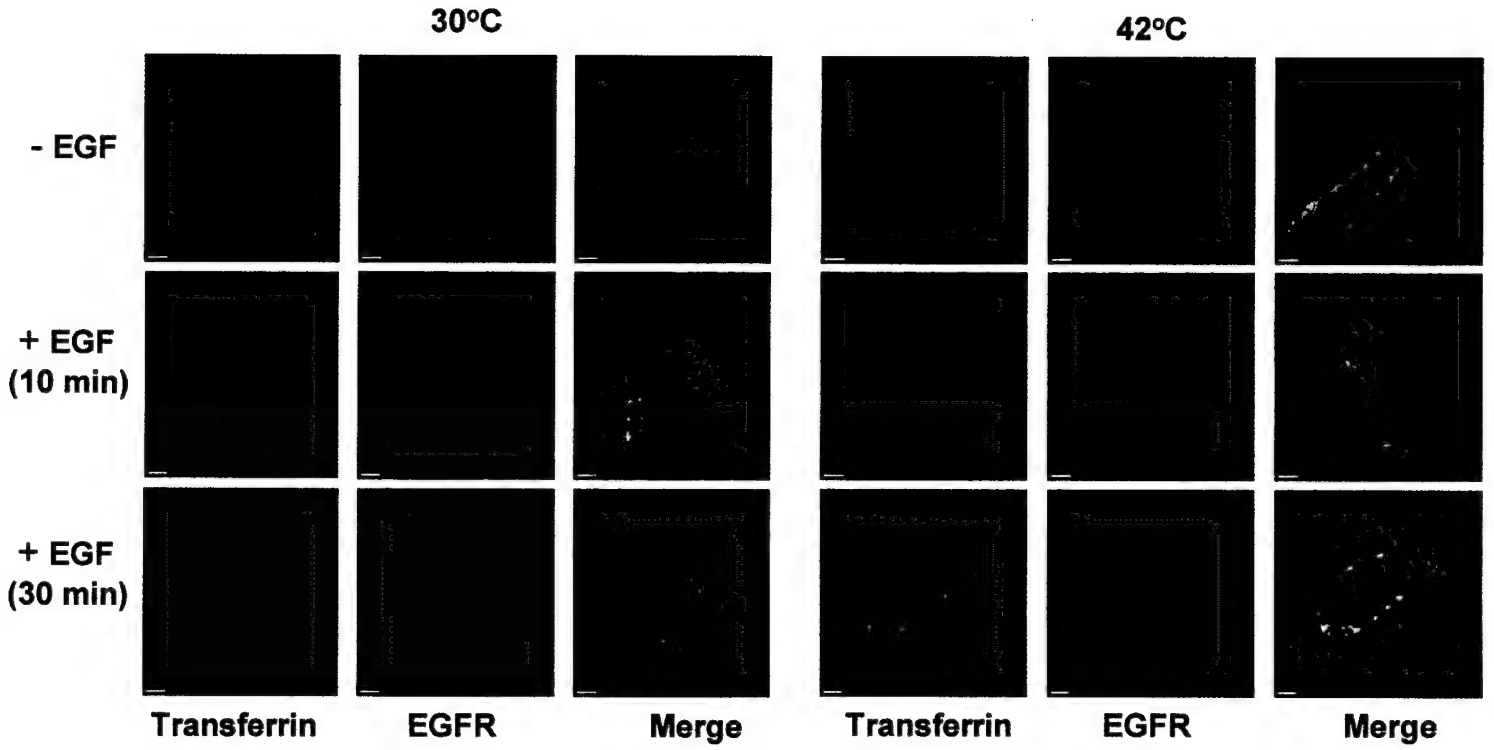

Figure 4. Prolonged colocalization of activated EGFR with transferrin (early and recycling endosome marker) upon temperature-dependent inhibition of ubiquitination in CHO-TS20 cells. TS20-EGFR cells were either maintained at permissive temperature (30˚C) or shifted to the non-permissive temperature (42˚C) for 4 hours. Cells were then left unstimulated or stimulated with EGF for 10 or 30 min. During the last 10 min of this incubation, cells were loaded with Fluo488 conjugated transferrin (green). Following EGF treatment, celled were fixed in 3.5% formaldehyde, permeablized with saponin and immunostained with anti-EGFR antibody followed by Cy3-conjugated goat anti-mouse antibody (red). Images were obtained using confocal microscopy (Leica TCS NT) with deconvolution and merged images were obtained electronically. Note that at 30˚C, EGFR and transferrin colocalization (seen at 10 min) is markedly lost at 30 min (reflecting EGFR movement to late endosomes). In contrast, EGFR and transferrin continue to colocalize at 30 min in cells grown at 42˚C reflecting a block of EGFR sorting to lysosomes

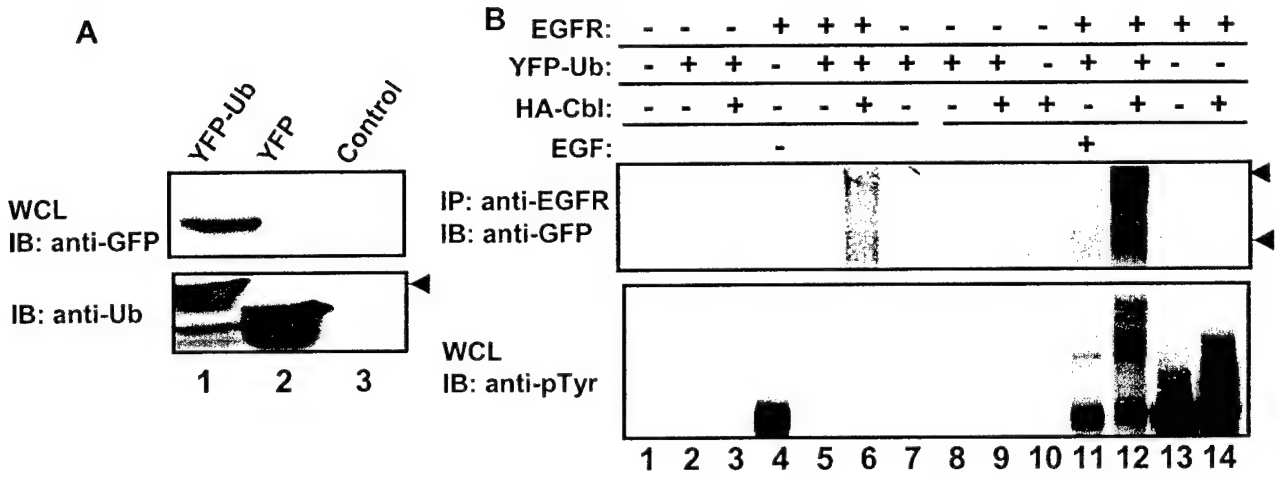

Figure 5. Generation of yellow fluorescent protein (YFP) tagged ubiquitin (YFP-Ub) and its use to demonstrate mono- and diubiquitination of EGFR. A. Ubiquitin, excised from pCDNA3.1-FLAG-Ub, was cloned into the pEYFP vector. Lysate from transfected 293T cells was immunoblotted with anti-GFP (which cross reacts with YFP) and anti-Ub antibodies to confirm expression. **B.** 293T cells were transfected with EGFR together with YFP-Ub and HA-Cbl as indicated, were then left unstimulated or stimulated with 100ng/ml EGF for 10 min. EGFR stimulation is visualized by blotting WCL with anti-pTyr antibody (lower panel). Anti-EGFR IPs were blotted with anti-GFP antibody to visualize YFP-modified EGFR (top panel). Two major bands corresponding to mono- and diubiquitinated EGFR (based on expected increase of size by ~32 KDa and 64 KDa) are indicated.

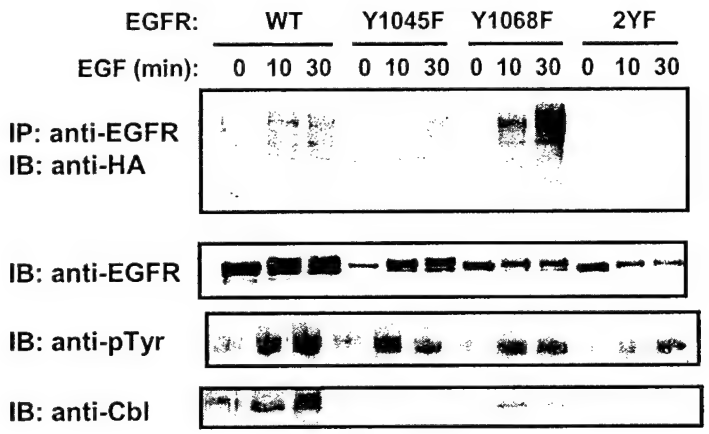

Figure 6. Mutation of the Cbl-TKB-binding site Y1045 blocks EGFR ubiquitination. 293T cells were transfected with the following EGFR constructs: wild type (WT), Y1045F, Y1068F and Y1045/1068 F (2YF). Cell were also transfected with GFP-Cbl and HA-ubiquitin (all lanes). 48 hr post-transfection, the cells were starved, in media containing 0.5% FBS for 4 hours, and either left unstimulated (0) or stimulated with EGF (100ng/ml) for the indicated times. Anti-EGFR IPs were blotted with anti-HA (top panel) and anti-EGFR (second panel). In a similar (but separate experiment), lysates were subjected to anti-EGFR IP and serially blotted with anti-Cbl (bottom panel) and anti-pTyr (third panel) antibodies. Note the marked reduction in Cbl association with Y1045F and 2YF mutants.

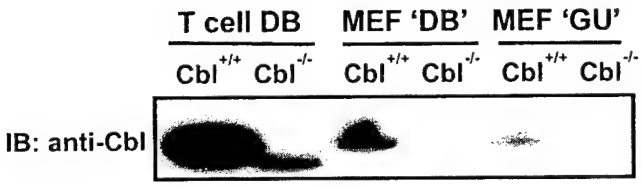

Figure 7. Demonstration of lack of Cbl expression in $Cbl^{-/-}$ mouse embryonic fibroblasts(MEFs) derived from $Cbl^{-/-}$ mice by Dr. David Bowtell (DB) and Dr. Hua Gu (GU). Lysate from T cell lines or MEFs from DB or HG were blotted with anti-Cbl antibody. Note the expected high expression of Cbl in T cells, allowing the detection of the truncated form of Cbl expressed in mice from this source. This band was also seen in MEF DB upon longer exposure, but no such bands are seen in MEF 'GU'.

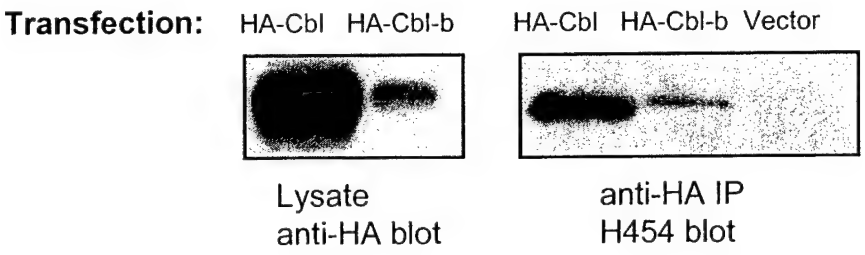

Fig. 8. Reactivity of H454 anti-Cbl-b antibody with both Cbl and Cbl-b. 293T cells were transiently transfected with pALTER-Max-HA-Cbl, pCDNA3-HA-Cbl-b or pcDNA3 vector and cell lysates or anti-HA immunoprecipitates were blotted with anti-HA and H454 (sc-1705, Santa Cruz Biotechnology, Inc.), respectively. H454 reacts with both Cbl and Cbl-b, proportionately with their levels of expression. We have further established this result using additional analyses using endogenous as well as transfected proteins (not shown).

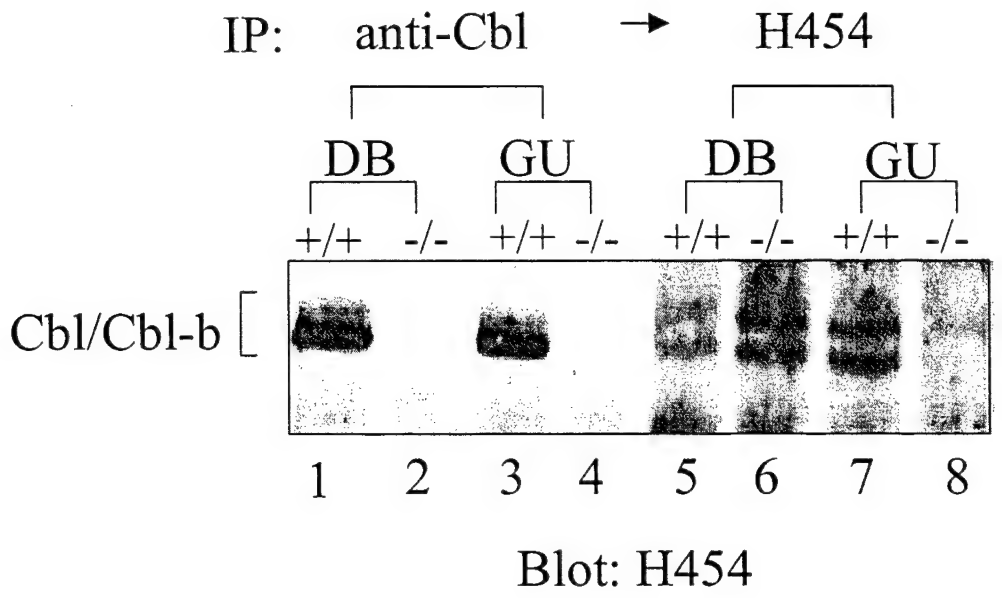

Figure 9. Assessment of Cbl-b protein expression in Cbl-/- MEFs using anti-Cbl/Cbl-b antibody H454. One mg aliquots of protein lysate were subjected to immunoprecipitation with anti-Cbl antibody (C15, Santa Cruz Biotechnology, Inc.) and these were resolved in lanes 1-4. The supernatants of these IPs were further subjected to anti-Cbl IP and found to be completely immunodepleted of Cbl (not shown). These Cbl-depleted lysates were subjected to a further IP with H454 antibody and these were resolved in lanes 6-8. The membrane was immunoblotted with H454 antibody to detect Cbl in lanes 1-4 and Cbl-b in lanes 5-8. Based on relatively equal reactivity of H454 antibody with Cbl and Cbl-b (seen in Addendum Figure 1), we estimate that Cbl-b represents less than 10% of total Cbl proteins in MEFs. Note that Cbl-b is undetectable in Cbl-/- GU MEF line (the reasons for this are unclear but make this line an essentially Cbl-null cell).

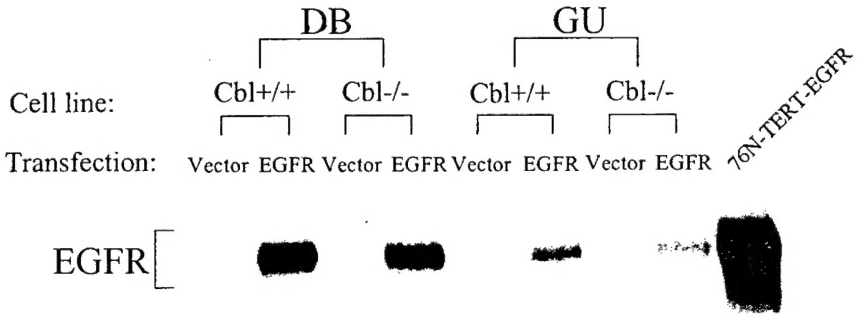

Blot: anti-EGFR

Fig. 10. Expression of retrovirally-transduced human EGFR in Cbl+/+ and Cbl-/- MEFs analyzed by immunoprecipitation and Western blotting. The indicated MEFs were infected with control retrovirus or a retrovirus encoding human EGFR (using the MSCV-puro-EGFR vector) and puromycin-resistant cell lines were established. Cells were serum-starved and Triton X-100 lysates were prepared. 200 ug aliquots of protein lysate were subjected to anti-EGFR immunoprecipitation (mAb 528), resolved by SDS-PAGE and immunoblotted with anti-EGFR antibody (Santa Cruz, sc003). Note the expression of human EGFR only in cells transduced with EGFR retrovirus. Telomerase-immortalized human mammary epithelial cell line 76N-TERT made to stably over-express human ErbB2 via retroviral infection was used for comparison.

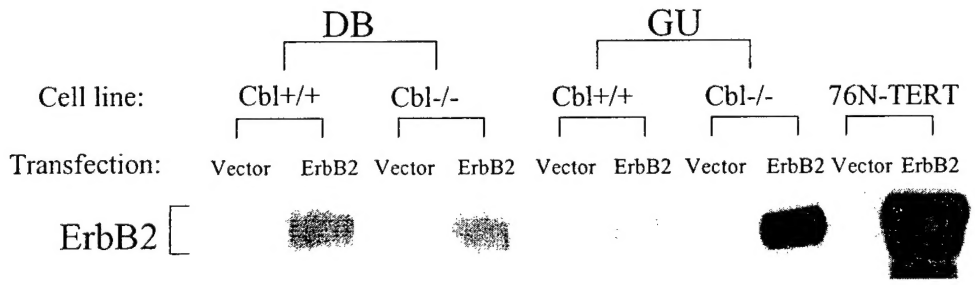

Blot: anti-ErbB2

Fig. 11. Expression of retrovirally-transduced human ErbB2 in Cbl+/+ and Cbl-/- MEFs analyzed by immunoprecipitation and Western blotting. The indicated MEFs were infected with control retrovirus or a retrovirus encoding human EGFR (using the MSCV-puro-EGFR vector) and puromycin-resistant cell lines were established. Cells were serum-starved and Triton X-100 lysates were prepared. 50 ug aliquots of protein lysate were resolved by SDS-PAGE and immunoblotted with an anti-ErbB2 antibody (Santa Cruz). Note the expression of human ErbB2 only in cells transduced with ErbB2 retrovirus. Telomerase-immortalized human mammary epithelial cell line 76N-TERT made to stably over-express human ErbB2 via retroviral infection and its vector control, were used for comparison.

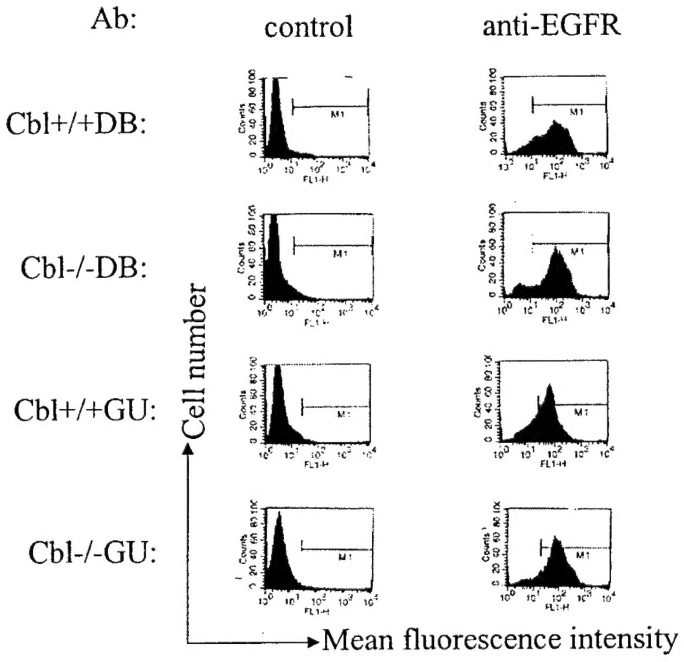

Fig. 12. Cell surface expression of retrovirally-transduced human EGFR on Cbl+/+ and Cbl-/- MEFs. The indicated MEFs were infected with retroviruses encoding human EGFR (using the MSCV-puro-EGFR vector) and puromycin-resistant cell lines were established. Immunostaining was performed with anti-EGFR antibody 528 or an isotype-matched control antibody for 45 minutes on ice. Cells were washed and stained with goat anti-mouse IgG-FITC conjugate for 30 minutes. Data were collected using a FACSort (BD) and analyzed using the CellQuest software. The cursors in each panel depict positively staining cells. Note that all transfected lines are nearly homogeneously EGFR-positive. Anti-EGFR staining of un-transfected MEFs was comparable to negative controls (not shown).

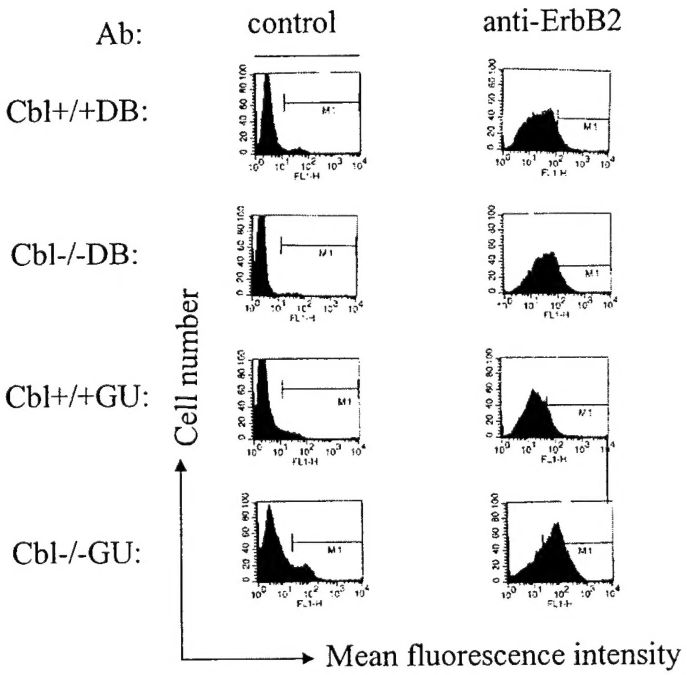

Fig. 13. Cell surface expression of retrovirally-transduced human ErbB2 on Cbl+/+ and Cbl-/- MEFs. The indicated MEFs were infected with retroviruses encoding human EGFR (using the MSCV-puro-ErbB2 vector) and puromycin-resistant cell lines were established. Immunostaining was performed with anti-ErbB2 monoclonal antibody (Santa Cruz Biotechnology) or an isotype-matched control antibody for 45 minutes on ice. Cells were washed and stained with goat anti-mouse IgG-FITC conjugate for 30 minutes. Data were collected using a FACSort (BD) and analyzed using the CellQuest software. The cursors in each panel depict positively staining cells. Note that all transfected lines are nearly homogeneously ErbB2-positive. Anti-ErbB2 staining of un-transfected MEFs was comparable to negative controls (not shown).